Nanosecond electric modification of order parameter in nematic and isotropic phases of materials with negative and positive dielectric anisotropy

Bing-Xiang Li[a,b], Volodymyr Borshch[a], Sergij V. Shiyanovskii[a], and Oleg D. Lavrentovich[a,*]
[a]Liquid Crystal Institute and Chemical Physics Interdisciplinary Program, Kent State University, Kent, Ohio 44242, USA
[b]College of Electronic and Information Engineering, Nanjing University of Aeronautics and Astronautics, Nanjing, Jiangsu 210016, China

ABSTRACT

We demonstrate nanosecond electro-optic switching in the nematic and isotropic phases of two nematic materials, one with a negative dielectric anisotropy (HNG715600-100) and another with a positive dielectric anisotropy (8CB). In both cases, the effect is caused by the nanosecond electric modification of the order parameter (NEMOP). In NEMOP effect, the electric field is applied in such a way that the director alignment is not distorted. The NEMOP effects in the nematic phases are compared to the Kerr effects of the isotropic phases of the same two materials. Although the amplitudes of NEMOP and Kerr effects are comparable, we observe differences in temperature dependencies. We also observe that the field-induced Kerr birefringence in the isotropic phases does not follow the expected quadratic dependence on the applied field. Namely, it grows slower in the dielectrically negative material and faster in the dielectrically positive material.

Keywords: nematic liquid crystals, negative dielectric anisotropy, positive dielectric anisotropy, nanosecond electric modification of order parameter, electro-optic response, Kerr effect, isotropic to nematic phase transition

1. INTRODUCTION

In a nematic liquid crystal (NLC), the molecules show orientational order along a certain direction in space, called the director $\hat{\mathbf{N}}(\mathbf{r})$, which is the optic axis of the material. Because of this orientational order, NLCs possess anisotropic physical properties, such as the dielectric anisotropy $\Delta\varepsilon = \varepsilon_{\parallel} - \varepsilon_{\perp}$ and birefringence $\Delta n = n_e - n_o$, where $\varepsilon_{\parallel}$ and $\varepsilon_{\perp}$ are the dielectric constants measured parallel and perpendicular to $\hat{\mathbf{N}}$, respectively; n_o and n_e are the ordinary and extraordinary refractive indices, respectively. A typical application of the NLCs (for example, in displays, optical switches) relies on realigning the director by an externally applied electric field. When the field is switched-off, the director relaxes back into a uniform state, as dictated by anisotropic molecular interactions at the bounding plates. The optical contrast is achieved because of birefringence. One of the principal difficulties is that the orientational relaxation of the director in the field-off state is a slow process limited by viscosity; the switch-off time is typically in the range of milliseconds[1]. This is why many research groups explore ways to reduce the switching time, by optimizing the viscoelastic parameters of the NLCs, using overdriving schemes of switching[1], and placing the NLCs into polymer networks[2].

Emerging Liquid Crystal Technologies X, edited by Liang-Chy Chien, Harry J. Coles, Hirotsugu Kikuchi, Ivan I. Smalyukh,
Proc. of SPIE Vol. 9384, 93840U · © 2015 SPIE · CCC code: 0277-786X/15/$18 · doi: 10.1117/12.2076657

Recently, we proposed a new approach to electro-optics of NLCs[3-5], called "nanosecond electric modification of order parameter" (NEMOP), by eliminating the process of director reorientation. The simplest realization is a NLC with negative anisotropy of dielectric permittivity subject to an electric field that is perpendicular to the director. Although the electric field does not reorient the director, it does cause other changes, by altering the degree of molecular order, the so-called order parameter[6]. These changes can be divided into three different categories. The first is the induction of biaxial order, with the secondary axis parallel to the field. The second effect is the modification of uniaxial order in the plane perpendicular to the field. Finally, the electric field also modifies the spectrum of director fluctuations[7-9]. The first two processes are extremely fast, developing within nanoseconds[3-5]. All three mechanisms change the effective birefringence of a material. An important and challenging task is to analyze their contributions separately. This separation can be achieved by varying the direction of the probing beam of light. For oblique incidence of probing beam, one can eliminate the contribution from the director fluctuations or the contribution from the biaxial order.

The nanosecond response in both the field-on and field-off switching of NEMOP is appealing for applications such as ultrafast electro-optics, quantum computing, secure communications. The issue of concern is that NEMOP requires relatively high electric fields and produces relatively low birefringence. Some of these problems can be overcome by a proper design of NLCs. For example, NLCs with strong anisotropy of dielectric and optical properties, show high NEMOP birefringence on the order of 10^{-2}, see Ref.5.

In this paper, we extend the NEMOP approach to other geometries, by exploring NLCs with a positive dielectric anisotropy and also comparing the effect to its counterpart in the isotropic phase. In the latter case, the electric field induces only uniaxial molecular order; the effect is known as the Kerr effect[10-13]. In Section 2, we discuss the theoretical background of the electrically modified order parameters in (i) a planar cell with $\Delta\varepsilon < 0$, (ii) homeotropic cell with $\Delta\varepsilon > 0$, and (iii) in the isotropic phase. Section 3 presents the experimental methods. Section 4 describes the experimental results for the three cases above.

2. THEORETICAL BACKGROUND

An NLC can be considered as a uniaxial medium with the director as the optic axis. In the laboratory frame $Oxyz$ with the z axis along the director, the field-free optic tensor $\tilde{\boldsymbol{\varepsilon}}^{(0)}$ of the NLC has the diagonal form $\left\{n_o^2, n_o^2, n_e^2\right\}$. An electric field applied in such a way that it does not realign the director, will modify the optic tensor $\tilde{\boldsymbol{\varepsilon}} = \tilde{\boldsymbol{\varepsilon}}^{(0)} + \delta\tilde{\boldsymbol{\varepsilon}}$ by creating the isotropic $\delta\tilde{\boldsymbol{\varepsilon}}_{iso}$, uniaxial $\delta\tilde{\boldsymbol{\varepsilon}}_u$, biaxial $\delta\tilde{\boldsymbol{\varepsilon}}_b$, and fluctuative $\delta\tilde{\boldsymbol{\varepsilon}}_f$ contributions:

$$\begin{aligned}
\delta\tilde{\varepsilon}_x &= \delta\tilde{\varepsilon}_{iso} - \frac{1}{3}\delta\tilde{\varepsilon}_u + \frac{1}{2}\delta\tilde{\varepsilon}_b - \delta\tilde{\varepsilon}_x^f, \\
\delta\tilde{\varepsilon}_y &= \delta\tilde{\varepsilon}_{iso} - \frac{1}{3}\delta\tilde{\varepsilon}_u - \frac{1}{2}\delta\tilde{\varepsilon}_b - \delta\tilde{\varepsilon}_y^f, \text{ and} \\
\delta\tilde{\varepsilon}_z &= \delta\tilde{\varepsilon}_{iso} + \frac{2}{3}\delta\tilde{\varepsilon}_u + \delta\tilde{\varepsilon}_x^f + \delta\tilde{\varepsilon}_x^f,
\end{aligned} \tag{1}$$

where

$$\delta\tilde{\varepsilon}_\alpha^f = -(\left\langle N_\alpha^2(t,\mathbf{r})\right\rangle - \left\langle N_\alpha^2(0,\mathbf{r})\right\rangle)(n_e^2 - n_o^2), \quad \alpha = x, y \tag{2}$$

In our experiments, the electric field stabilizes the director and, therefore, decreases $\left\langle N_\alpha^2(t,\mathbf{r})\right\rangle$; we chose the sign in Eq. (2) to make $\delta\tilde{\varepsilon}_\alpha^f \geq 0$.

2.1 Negative dielectric materials in planar geometry

When an electric field is applied along the *x* axis, perpendicular to the director of an NLC with $\Delta\varepsilon < 0$, the electric field only affects the director fluctuations along the x axis, $\delta\tilde{\varepsilon}_y^f = 0$.

We describe optic properties using the normalized wavevectors $\tilde{\mathbf{k}} = \frac{\lambda \mathbf{k}}{2\pi}$ of the optical modes, where λ is the wavelength of a probing beam in vacuum. The tangential components $\tilde{k}_y$ and $\tilde{k}_z$ are preserved at interfaces between different layers (glass, ITO, polymer, nematic, etc.), and are the same for all optical modes. The optical retardance between the two forward modes propagating through the field-induced (effectively biaxial) states of the NLC, $\Gamma = \Delta n_{eff} d$, is determined by the NLC thickness d and the effective birefringence $\Delta n_{eff} = \tilde{k}_x^{(1)} - \tilde{k}_x^{(2)}$, where $\tilde{k}_x^{(1)}$ and $\tilde{k}_x^{(2)}$ are solutions of the Fresnel equation for two forward propagating modes, $\tilde{k}_x > 0$ in the biaxial medium:

$$\tilde{\varepsilon}_x \tilde{k}_x^4 - Q_2 \tilde{k}_x^2 + Q_0 = 0\,, \tag{3}$$

where $Q_2 = \tilde{\varepsilon}_x(\tilde{\varepsilon}_y + \tilde{\varepsilon}_z) - \tilde{k}_y^2(\tilde{\varepsilon}_x + \tilde{\varepsilon}_y) - \tilde{k}_z^2(\tilde{\varepsilon}_x + \tilde{\varepsilon}_z)$ and $Q_0 = (\tilde{\varepsilon}_y\tilde{\varepsilon}_z - \tilde{\varepsilon}_y\tilde{k}_y^2 - \tilde{\varepsilon}_z\tilde{k}_z^2)(\tilde{\varepsilon}_x - \tilde{k}_y^2 - \tilde{k}_z^2)$. In the field-free uniaxial state, modes 1 and 2 are the extraordinary $\tilde{k}_x^{(1)} = \tilde{k}_{xe} = \sqrt{n_e^2(1 - \tilde{k}_z^2/n_o^2) - \tilde{k}_y^2}$ and ordinary $\tilde{k}_x^{(2)} = \tilde{k}_{xo} = \sqrt{n_o^2 - \tilde{k}_y^2 - \tilde{k}_z^2}$ waves, respectively. The applied electric field changes the effective birefringence $\delta n_{eff} = (\tilde{k}_x^{(1)} - \tilde{k}_{xe}) - (\tilde{k}_x^{(2)} - \tilde{k}_{xo})$, calculated from Eq. (3) as

$$\delta n_{eff} = \frac{\delta\tilde{\varepsilon}_x(\tilde{k}_z^2\tilde{k}_{xe}\tilde{k}_{xo} - \tilde{k}_y^2 n_o^2) + \delta\tilde{\varepsilon}_y(\tilde{k}_y^2\tilde{k}_z^2\tilde{k}_{xo} - \tilde{k}_{xe}n_o^2\tilde{k}_{xo}^2) + \delta\tilde{\varepsilon}_z(n_o^2 - \tilde{k}_z^2)\tilde{k}_{xo}}{2\tilde{k}_{xe}\tilde{k}_{xo}n_o^2(n_o^2 - \tilde{k}_z^2)}\,. \tag{4}$$

Using Eq. (1) for the discussed contributions, we obtain from Eq. (4)

$$\delta n_{eff} = \sigma_{bu}(\delta\tilde{\varepsilon}_u + \frac{3}{2}\delta\tilde{\varepsilon}_b) + \sigma_{uf}(\delta\tilde{\varepsilon}_u + \frac{3}{2}\delta\tilde{\varepsilon}_f)\,, \tag{5}$$

where $\sigma_{bu} = \frac{1}{6n_o^2(n_o^2 - \tilde{k}_z^2)}\left[\tilde{k}_z^2(\tilde{k}_{xe} - \frac{\tilde{k}_y^2}{\tilde{k}_{xe}}) + n_o^2(\tilde{k}_{xo} - \frac{\tilde{k}_y^2}{\tilde{k}_{xo}})\right]$ and $\sigma_{uf} = \frac{1}{3n_o^2}\left[\frac{n_o^2 - \tilde{k}_z^2}{\tilde{k}_{xe}} + \frac{\tilde{k}_y^2 n_o^2 - \tilde{k}_z^2\tilde{k}_{xo}\tilde{k}_{xe}}{\tilde{k}_{xo}(n_o^2 - \tilde{k}_z^2)}\right]$ are the weighting coefficients dependent on the experimental geometry. Note that $\delta\tilde{\varepsilon}_{iso}$ does not contribute to δn_{eff}.

We perform experiments for the following two geometries that provide the simplest interpretation:

(a) "Biaxial-uniaxial" (BU) geometry, in which the contribution of director fluctuations is eliminated, $\sigma_{uf} = 0$, by choosing $\tilde{k}_y = 0$, and $\tilde{k}_z = n_o^2 \Big/ \sqrt{n_e^2 + n_o^2}$. The field-induced change δn_{BU} for this BU geometry is

$$\delta n_{BU} = \frac{n_o/n_e + 1 + n_e/n_o}{6\sqrt{n_e^2 + n_o^2}}\left(\delta\tilde{\varepsilon}_u + \frac{3}{2}\delta\tilde{\varepsilon}_b\right). \tag{6}$$

(b) "Uniaxial-fluctuative" (UF) geometry: $\sigma_{bu} = 0$, by choosing $\tilde{k}_z = 0$, and $\tilde{k}_y = n_o / \sqrt{2}$. The corresponding field-induced birefringence δn_{UF} is

$$\delta n_{UF} = \frac{1}{3\sqrt{2}} \left(\frac{1}{n_o} + \frac{2}{\sqrt{2n_e^2 - n_o^2}} \right) \left(\delta\varepsilon_u + \frac{3}{2} \delta\varepsilon_u \right). \tag{7}$$

If the refractive indices of NLC n_e and n_o are close to the refractive index of the glass substrate, then the incident angles in BU and UF geometries are close to $45°$.

2.2 Positive dielectric materials in homeotropic geometry

The electric field applied along the director of a NLC with $\Delta\varepsilon > 0$ in a homeotropic cell does not change the uniaxial geometry of the NLC, $\delta\tilde{\varepsilon}_b = 0$, and affects equally the director fluctuations along the x and y axes, $\delta\tilde{\varepsilon}_x^f = \delta\tilde{\varepsilon}_y^f = \delta\tilde{\varepsilon}_f$.

In the laboratory frame $Oxyz$, we choose the x axis perpendicular to the director and in the incident plane, $\tilde{k}_y = 0$. The two forward-propagating modes $\tilde{k}_z^{(1)}$ and $\tilde{k}_z^{(2)}$ are the extraordinary $\tilde{k}_z^{(1)} = \tilde{k}_e = \sqrt{\varepsilon_x (1 - \tilde{k}_x^2 / \varepsilon_z)}$ and ordinary $\tilde{k}_z^{(2)} = \tilde{k}_o = \sqrt{\varepsilon_x - \tilde{k}_x^2}$ waves, respectively. In the geometry where the angle between the director and the laser beam is about $45°$ ($\tilde{k}_x = n_o / \sqrt{2}$), the field induced effective birefringence of the NLC in the homeotropic cell is

$$\delta n_h = \frac{\delta\tilde{\varepsilon}_u + 3\delta\tilde{\varepsilon}_f}{3} \left(\frac{n_e^2 n_o^2 - 2n_e^4 + 2n_o^4 + 2n_e^3 \sqrt{2n_e^2 - n_o^2}}{2n_e^3 n_o \sqrt{4n_e^2 - 2n_o^2}} \right). \tag{8}$$

2.3 NLCs in the Isotropic phase

In the isotropic phase, the applied electric field induces a uniaxial orientational order along the field, so that $\delta\tilde{\varepsilon}_b = 0$ and $\delta\tilde{\varepsilon}_x^f = \delta\tilde{\varepsilon}_y^f = 0$ in Eq. (1). When the probing beam is directed at 45° with respect to the applied electric field, one can use Eq.(8) with $n_e = n_o = n_{iso}$ and $\delta\tilde{\varepsilon}_f = 0$, to calculate the field induced effective birefringence of the isotropic phase as

$$\delta n_{iso} = \frac{\sqrt{2}\delta\tilde{\varepsilon}_u}{4n_{iso}} \tag{9}$$

For materials formed by molecules with a transverse dipole ($\Delta\varepsilon < 0$ in the nematic phase), the applied electric field reorients the short axes of the molecules predominantly along the induced director, $\delta\tilde{\varepsilon}_u < 0$; as a result, $\delta n_{iso} < 0$. In contrast, for materials with $\Delta\varepsilon > 0$, the molecules prefer to align along the field, $\delta\tilde{\varepsilon}_u > 0$, so that $\delta n_{iso} > 0$.

3. MATERIALS AND EXPERIMENTAL METHODS

We used two commercial NLCs, HNG715600-100 ($\Delta\varepsilon < 0$, purchased from Jiangsu Hecheng Display Technology) and 4-n-octyl-4′-cyanobiphenyl (8CB) ($\Delta\varepsilon > 0$, purchased from Merck). The material parameters of HNG715600-100 measured at 25˚C are as follows: $\Delta\varepsilon = -12.2$, $\Delta n = 0.153$, the nematic phase exists in the temperature range from -30 to 88˚C. HNG715600-100 was injected into a planar cell (rubbed polyimide PI-2555, HD MicroSystems) of thickness 5.1 μm. The material parameters of 8CB measured at 34˚C are as follows: $\Delta\varepsilon = 7.6$, $\Delta n = 0.153$, the nematic temperature range is from 32.5 ˚C to 40˚C. The homeotropic cells filled with 8CB (polyimide SI-1211, Nissan Chemicals) were 4.6-5 μm thick.

All cells have low resistivity (about 10 Ω/sq) indium tin oxide (ITO) electrodes of active area 2×2 mm^2. The cell is sandwiched between two right-angled prisms in the holder. The temperature of the cell assembly is controlled with a Linkam LTS350 hot stage and a Linkam TMS94 controller. The voltage pulse is applied using a pulse generator HV1000 (Direct Energy), which allows fast rise and fall characteristic times, τ ~ 3.2 ns. The light intensity is measured using a photodetector TIA-525 (Terahertz Techonologies). The applied voltage pulses and photodetector signals are measured with 1G sample/s digital oscilloscope TDS2014 (Tektronix). The same setup described in Refs. 3-5 is used to measure the optical response, Fig. 1.

Dynamics of field-induced birefringence $\delta n(t)$ in response to the voltage pulses was determined by measuring the intensity $I(t)$ of a He-Ne laser beam (wavelength λ = 633nm):

$$I(t) = I_0 \sin^2\left(\frac{\sqrt{2}\pi d\left(\delta n(t) + \Delta n_{eff}\right)}{\lambda} + \frac{\varphi_{SB}}{2}\right), \tag{10}$$

where Δn_{eff} is the effective birefringence; φ_{SB} is the additional controlled phase difference, I_0 is the intensity of light impinging on the NLC cell.

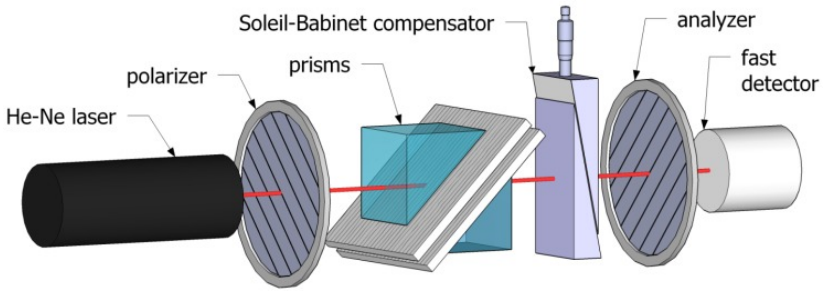

Figure 1. Experimental setup: A test cell sandwiched between two right angle prisms, probed with a linearly polarized laser beam that propagates inside the nematic slab at the angle 45 with respect to the cell normal.

4. EXPERIMENTAL RESULTS AND DISCUSSIONS

4.1 Negative dielectric materials HNG715600-100 in planar geometry

The NLCs with $\Delta\varepsilon < 0$ exhibit two fast processes of NEMOP response (nanosecond biaxial and uniaxial modifications of order parameter) and a relatively slow quenching of the director fluctuations (up to milliseconds)[3-4]. The most studied NLC material of this type, CCN-47, exhibits a narrow nematic temperature range and small field-induced birefringence, Fig. 2, which limits its practical applications. Investigating the NEMOP effect in a variety of NLCs with $\Delta\varepsilon < 0$, we found that one of the best mixtures is HNG715600-100, which demonstrates the nematic phase at wide range of

temperatures, including the room temperature, and shows the amplitude of NEMOP birefringence that is one order of magnitude larger than CCN-47. Below, we present a detailed description of the NEMOP effect in HNG715600-100.

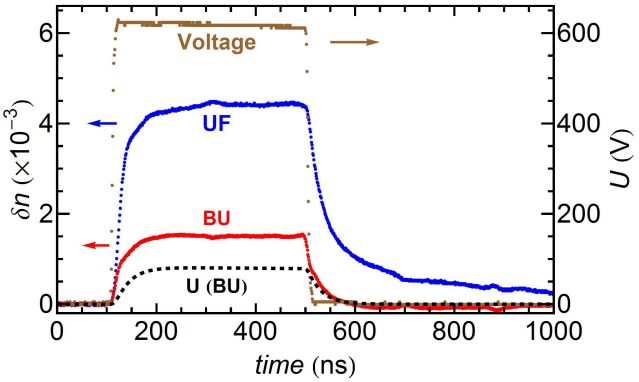

Figure 2. Dynamics of the field-induced birefringence of the NLC material CCN-47 in response to the applied voltage pulse of amplitude 626 V at 49°C for BU (red dots) and UF (blue dots) geometries. The black dashed line represents the uniaxial contribution of the optical response in BU geometry; the uniaxial contribution in UF geometry is twice lager than that in BU, compare Eqs. (6) and (7).

Fig. 3(a) shows the NEMOP response in the BU geometry, for four different temperatures within the NLOC. The optical response occurs within tens of nanoseconds. The maximum induced birefringence $\delta n_{\max}$ is higher at low temperatures. In the UF geometry, Fig. 3(b), the response time is shorter at high temperatures and the switch-on process is faster than the switch-off process. These features of UF geometry are caused by quenching of director fluctuations. Interestingly, at high temperature 80°C, the field induced birefringence becomes negative after the field is switched off; this effect might be related to the presence of different components in the HNG715600-100 mixture.

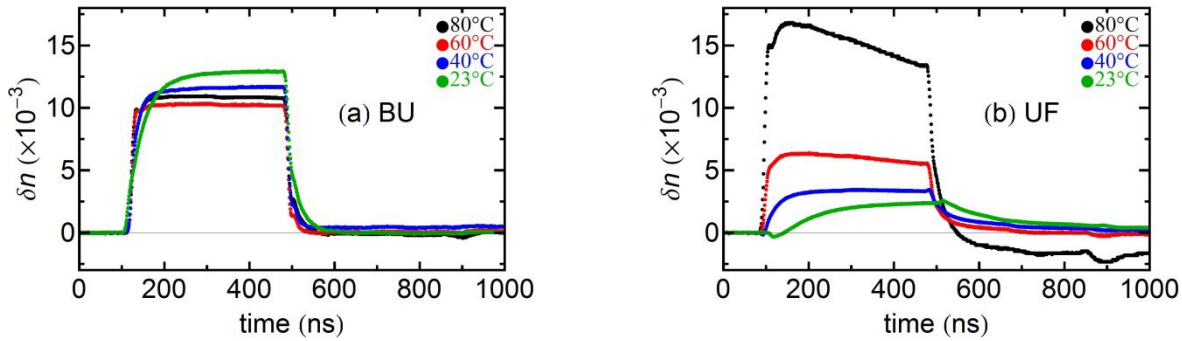

Figure 3. The dynamics of the field-induced birefringence of HNG715600-100 in response to the applied electric field of amplitude E=1.3×10^8 V/m at various temperatures for (a) BU (the curve at 400 ns from top to bottom represent 23°C, 40°C, 80°C, and 60°C respectively) and (b) UF (the curve at 400 ns from top to bottom represent 80°C, 60°C, 40°C, and 23°C, respectively) geometries.

The behavior of the isotropic phase of HNG715600-100 (Kerr effect) is shown in Fig. 4. The switch-on process is noticeably faster than the switch-off process. The switch off time increases from tens of nanoseconds to hundreds of nanoseconds as the temperature drops from 121°C to 93°C. For the same temperature change, the field-induced birefringence increases by a factor of 5. These temperature dependencies are expected for the Kerr effect; their existence complicates practical applications of the Kerr effect.

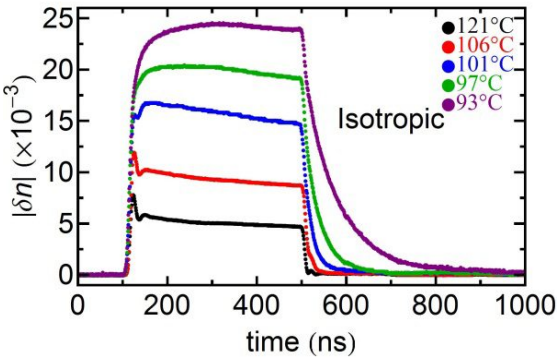

Figure 4. The dynamics of the field-induced birefringence of HNG715600-100 in response to the applied electric field of amplitude E=1.3×10^8 V/m at various temperatures in the isotropic phase. The curve at 400 ns from top to bottom represent 93°C, 106°C, 101°C, 97°C, and 121°C, respectively.

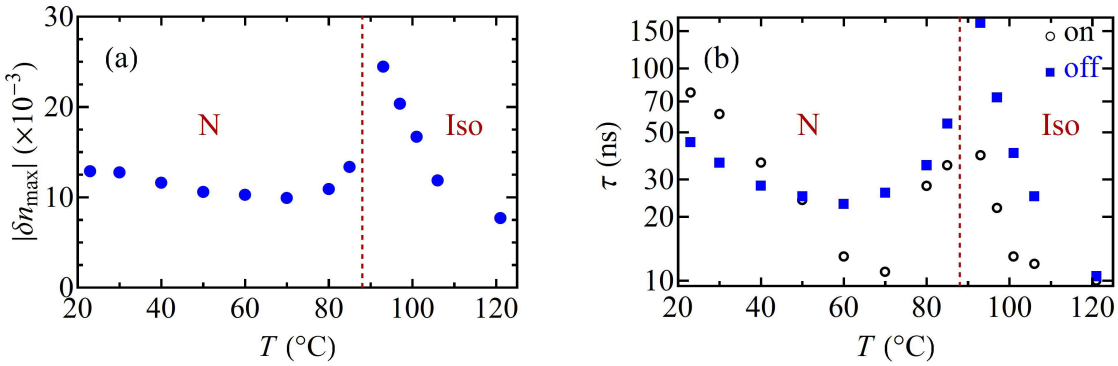

Figure 5. Temperature dependence of (a) amplitude of the field-induced birefringence and (b) switch-on and switch-off times of HNG715600-100 at E=1.3×10^8 V/m measured in BU geometry.

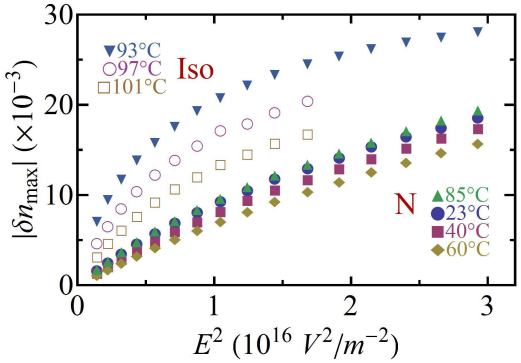

Figure 6. Electric dependence of amplitude of the field-induced birefringence of HNG715600-100 at various temperatures.

Comparison of the amplitudes of field-induced birefringence in NEMOP and Kerr effects for HNG715600-100 mixture is presented in Fig. 5(a). The amplitude of optical response in the isotropic phase close to the temperature T_{NI} of the isotropic-nematic transition is generally several times larger than that in the nematic phase. The reason is that the field-free order parameter of the isotropic phase is zero, thus the electric field can induce a relatively large order parameter. Although the induced birefringence is higher in the isotropic phase, the advantage of the nematic phase is that the optical

response show weaker temperature dependence, both in terms of birefringence, Fig.5 (a), and the switch-off response time, Fig. 5(b); the response times (at E=1.3×10^8 V/m) are calculated using the 10% - 90% criterium.

According to the theory of Kerr effect and the NEMOP effect, the amplitude of the field-induced birefringence should grow as E^2. Figure 6 shows that the behavior of HNG715600-100 does not generally follow this expectation. Both in the isotropic phase and in the nematic phase, the field-induced birefringence grows slower than E^2, Fig. 6. These features might be related to the high-order terms in the Landau-de Gennes model: the field-induced order parameter is negative, thus the negative third order term with the coefficient B in the Landau-de Gennes model decreases its value.

4.2 Positive dielectric materials 8CB in homeotropic geometry

We choose a single component material 8CB with a field-free birefringence similar to that of HNG715600-100 in order to compare the NEMOP effects in materials with $\Delta\varepsilon > 0$ and $\Delta\varepsilon < 0$, Fig.7-9. To avoid the electric breakdown, the electric field was limited by 7.2×10^7 V/m.

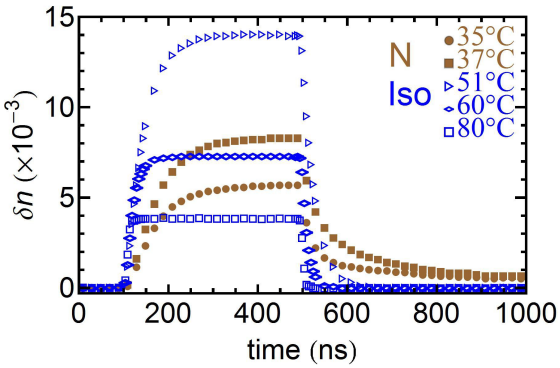

Figure 7. The dynamics of the field-induced birefringence of 8CB in response to the applied electric field of amplitude E = 6.5×10^7 V/m at various temperatures both in the nematic and isotropic phases.

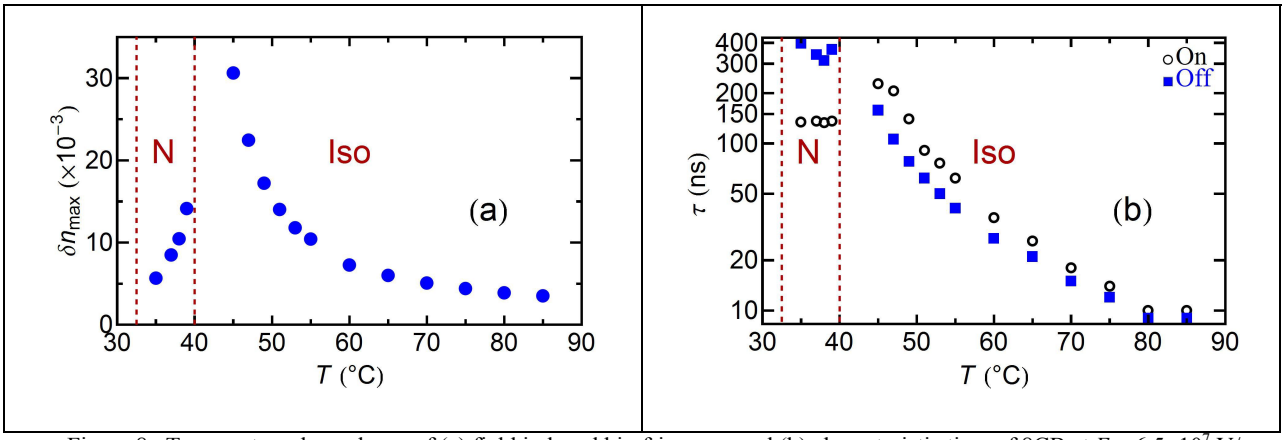

Figure 8. Temperature dependence of (a) field induced birefringence and (b) characteristic time of 8CB at E = 6.5×10^7 V/m.

In the nematic phase of 8CB, the NEMOP response occurs within hundreds of nanoseconds, Fig.7, 8(b). This relatively slow relaxation is caused by quenching of the director fluctuations. The field-induced birefringence is comparable to that of HNG715600-100. It increases with temperature and is higher in the isotropic phase as compared to the nematic phase, Fig.7 and 8(a).

Figure 9 shows that the behavior of 8CB does not generally follow the behavior expected from the standard theory of the Kerr effect. Namely, near the phase transition in the isotropic phase, the field-induced birefringence grows faster than E^2, Fig.9. This behavior might be again related to the third order term in the Landau-de Gennes model.

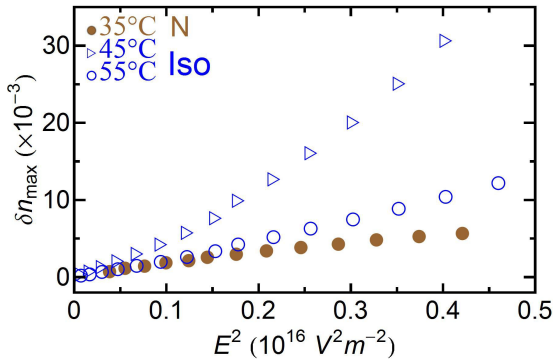

Figure 9. The field-induced birefringence of 8CB as function of the square of the applied electric field.

5. CONCLUSIONS

We investigated the nanosecond electro-optic switching in the nematic and isotropic phases of the NLC materials with negative and positive dielectric anisotropy. In both cases, the electric field was applied to leave the director orientation intact and to modify only the degree of orientational order. We studied the response in the so-called biaxial-uniaxial (BU) geometry, in which the effect of the slow process of director fluctuations quenching is eliminated from the optical response. In addition, we explored the uniaxial-fluctuations (UF) geometry, in which the optical response is caused mainly by the uniaxial modification of the order parameters and quenching of the director fluctuations. In BU geometry, the field induced birefringence of the planar cells of nematic HNG715600-100 with $\Delta\varepsilon < 0$ exhibits tens-of-nanoseconds response time and relatively weak temperature dependence over a broad (60°C) temperature range, including the room temperature. The weak temperature dependence of the NEMOP effect represents an attractive feature as compared to the Kerr effect in the isotropic phase. We also demonstrate the NEMOP response in a different geometry of homeotropic cells filled with a $\Delta\varepsilon > 0$ material, 8CB. The field-induced birefringence in the nematic phase of 8CB is comparable to that one observed in HNG715600-100. Since the latter represents the best NEMOP $\Delta\varepsilon < 0$ material from 13 studied so far, this result suggests that dielectrically positive materials in general might be very promising in terms of enhancement of the NEMOP response, especially in the case of a wide temperature range of the nematic phase. Comparison of the NEMOP effect in the nematic phase of 8CB to the Kerr effect in the isotropic phase of the same material shows that generally, near the phase transition, the isotropic phase shows a larger field-induced birefringence, but the strong temperature dependence complicates practical applications of the effect. An interesting feature of the Kerr response observed in our work is that the field-induced birefringence does not follow the expected E^2 dependency. Namely, in the isotropic phase of HNG715600-100, the birefringence grows more slowly than E^2, while in the isotropic phase of 8CB with $\Delta\varepsilon > 0$, the birefringence grows faster than E^2. The mechanisms of this departure from the classic model deserve further studies; tentatively, they can be associated with the third order term in the Landau-de Gennes model of the nematic-isotropic phase transition.

ACKNOWLEGMENT

The work was supported by State of Ohio through Ohio Development Services Agency and Ohio Third Frontier grant TECG20140133, and by China Scholarship Council. The content of this publication reflects the views of the authors and does not purport to reflect the views of Ohio Development Services Agency and/or that of the State of Ohio.

REFERENCES

[1] Yang, D. -K. and Wu, S.-T., [Fundamentals of Liquid Crystal Devices], John Wiley, New York (2006).
[2] Xiang, J. and Lavrentovich, O. D., "Blue-phase-polymer-templated nematic with sub-millisecond broad-temperature range electro-optic switching", Appl. Phys. Lett. **103**, 051112 (2013).
[3] Borshch, V., Shiyanovskii, S. V., and Lavrentovich, O. D., "Nanosecond Electro-Optic Switching of a Liquid Crystal", Phys. Rev. Lett. **111**, 107802 (2013).
[4] Borshch, V., Shiyanovskii, S. V., Li, B. -X., and Lavrentovich, O. D., "Nanosecond electro-optics of a nematic liquid crystal with negative dielectric anisotropy", Phys. Rev. E. **90**, 062504 (2014).
[5] Li, B.-X., Borshch, V., Shiyanovskii, S. V., Liu, S.-B., and Lavrentovich, O. D., "Electro-optic switching of dielectrically negative nematic through nanosecond electric modification of order parameter", Appl. Phys. Lett. **104**, 201105 (2014).
[6] de Gennes, P. G. and Prost, J., [The Physics of Liquid Crystals], Clarendon Press; Oxford University Press, Oxford, New York, p. 58 (1995).
[7] Kleman, M. and Lavrentovich, O.D., [Soft Matter Physics: An Introduction], Springer, New York, London, p. 171 (2003).
[8] Dunmur, D. A., Waterworth, T. F., and Palffy-Muhoray, P., "Electric Field Induced Birefringence in Nematic Liquid Crystal Films: Evidence for Wall Quenching of Director Fluctuations", Mol. Cryst. Liq. Cryst. **124**, 73 (1985).
[9] Dunmur, D. A. and Szumilin, K., "Field quenching of director fluctuations in thin films of nematic liquid crystals", Mol. Cryst. Liq. Cryst. **6**, 449-455 (1989).
[10] Johnston, Alan R., "Kerr response of nematic liquids", J. Appl. Phys. **44**, 2971-2974 (1973).
[11] Lelidis, I. and Durand, G., "Electrothermal effect in nematic liquid crystal", Phys. Rev. Lett. **76**(11), 1868 (1996).
[12] Schneider, L. and Wendorff, J. H., "Kerr effect studies on mixtures of liquid crystals", Liq. Cryst., **22**(1), 29 (1997).
[13] Filippini, J. C. and Poggi, Y., "Temperature dependence of the Kerr effect response time of nematogenic liquids", Phys. Lett. A **65**(1), 30 (1978).